2024 IEEE International Conference on Robotics and Automation (ICRA 2024)
May 13-17, 2024. Yokohama, Japan

Bicode: A Hybrid Blinking Marker System for Event Cameras

Takuya Kitade[1,2], Wataru Yamada[1], Keiichi Ochiai[1] and Michita Imai[2]

Abstract— **In the field of robotics, tag systems play an important role in various applications, such as object identification and robot control in real-world environments. While typical visual markers use two-dimensional (2D) patterns and RGB cameras for recognizing object IDs and poses, achieving long-distance recognition necessitates increasing marker size and camera magnification to ensure the required resolution. Furthermore, the growing adoption of event cameras in robotics captures rapid changes in pixel brightness but faces limitations in recognizing stationary 2D markers. Although compact blinker markers using blinking light-emitting diodes (LEDs) achieve long-distance recognition, they are constrained by the number of IDs or recognition speed when used with standard RGB cameras. In addition, recognizing object pose using only a single blinking LED presents challenges. To address these challenges, we introduce 'Bicode,' an indoor visual marker designed for event cameras. Bicode seamlessly integrates 2D and blinker markers within a single marker unit. We have developed prototypes of 2.5, 5, and 10 cm square acrylic 2D markers, each equipped with a single LED blinking at 1 kHz, enabling recognition with an event camera. Our experiments revealed the effects of marker size, LED light quantity, recognition distance, and angle, external lighting conditions, and camera or marker movement on accuracy. Notably, using the 5 cm marker, we confirmed its compatibility to recognize IDs at distances exceeding 20 m, and pose recognition at 2.5 m was confirmed.**

I. INTRODUCTION

In the field of robotics, tag systems are widely used for tasks such as object detection for interaction and robot control within real-world environments such as offices and warehouses. Several tag methods have been explored, including electromagnetic techniques, such as radio frequency identification [1]–[6], Bluetooth [7], [8], and magnetic force [9]–[12]. In addition, visual markers using cameras have been proposed. To enable robots to recognize their surroundings and objects for applications such as simultaneous localization and mapping and object detection, cameras are often integrated into robotic systems. Thus, visual markers serve as a common tag system that uses cameras. Since the robot moves around, its onboard camera needs to capture objects and their environment in a vast space at high speed. To achieve high-speed motion capture with low computational complexity, researchers have been investigating event cameras, which asynchronously capture pixels only when changes in luminance occur at high speed, on the order of microseconds [13]–[19]. In this paper, we propose a novel visual marker system designed for event cameras and capable of rapid ID detection in expansive indoor spaces and pose estimation when the robot is in proximity.

[1]NTT DOCOMO, INC., Tokyo, Japan {takuyakitade | wataruyamada | keiichi.ochiai}@acm.org
[2]Keio University, Yokohama, Japan michita@keio.jp

2D marker systems [20]–[24], which have a 2D pattern printed on various surfaces, are studied as visual markers that can accurately recognize marker IDs and poses using RGB cameras. Sarmadi et al. proposed a system that can track moving 2D markers with an event camera, focusing on the edges of the markers as they move [25]. These systems offer the advantage of recognizing the ID and pose using inexpensive markers and cameras. However, their recognition range depends on the clarity of the captured 2D pattern. To extend the recognition distance, it becomes necessary to either increase the camera magnification, enhance resolution, or enlarge the size of the camera marker.

Therefore, a visual marker system that can recognize objects from a distance, although small, using bright spots, such as LEDs, has been proposed. In the Bokode system [26], the use of a tiny 2D marker within an LED enables recognition at a long distance using the bokeh of the camera. However, the camera focus must be set to infinity, which limits the camera's use. Another technique using small bright spots is a blinker marker system in which IDs are superimposed on blinking light sources [27]–[29]. The blinker marker system requires only the ability to capture bright blinking spots and can recognize even small dots in an image. Therefore, ID recognition is possible from a distance even with a small blinker marker. However, 2D marker systems can recognize poses from the spatial pattern, while a single blinker marker is only a point on the image, making it unable to recognize poses without combining multiple blinker markers. In addition, 2D markers can be recognized from at least one frame, whereas blinker markers can be recognized from multiple frames. Consequently, the ID transmission rate of the blinker marker relies on the frame rate of the camera, leading to its limitations in the number of IDs that can be transmitted or potentially longer recognition times. For instance, if a camera operating at $30\,\mathrm{fps}$ is used to transmit 1 bit of data in each frame, the resulting data rate would be $30\,\mathrm{bps}$.

Although the method for blinking the 2D marker itself [30], [31] enhances ID recognition over longer distances and allows for the recognition of 2D marker patterns, such as nearby poses, it still faces a limitation in terms of blinker ID transfer speed when using general RGB cameras. In contrast, Censi et al. [32] achieved the recognition of blinker markers at a rapid rate of $1\,\mathrm{kHz}$ by using an event camera. However, for pose recognition, multiple blinking markers become necessary. Consequently, a challenge remains in achieving compatibility between pose recognition and high-speed ID recognition within a small blinker marker.

In this paper, we propose a novel indoor marker system named 'Bicode.' Bicode is designed to be detectable from

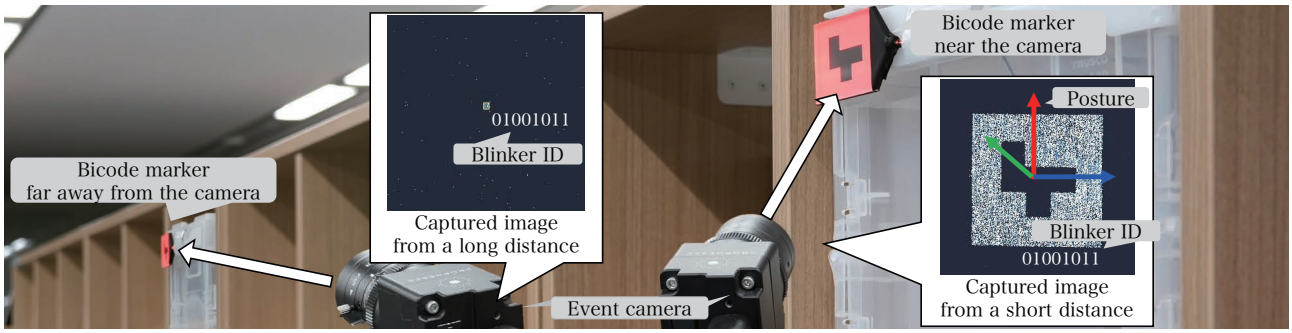

Fig. 1. Bicode marker concept: The figure illustrates the recognition process of Bicode markers by the event camera. A Bicode marker that is close to the camera is recognized as a blinker and 2D marker, whereas a Bicode marker that is far away from the camera is recognized solely as a blinker marker.

a distance using wideband IDs while also being capable of recognizing pose when a camera is in proximity to the marker. The core concept of our method involves integrating a rapid and wideband blinker marker feature into a small 2D marker and capturing it using an event camera. The 2D marker is illuminated by a blinking LED with an ID superimposed, blinking at a rate of approximately $1\,\mathrm{kHz}$. These combined markers are captured by an event camera to be analyzed frame by frame for 2D marker recognition and overtime for blinker marker recognition.

Fig. 1 illustrates the concept of Bicode. When the marker is far away from the camera, it is recognized as a blinker marker. However, when it is close to the camera, it works as a blinker and 2D markers. This system achieves these capabilities using a small marker, which traditionally would require either a large 2D marker or multiple blinker marker. Furthermore, using an event camera, Bicode can recognize wideband IDs. Therefore, our system has the potential to detect a large number of objects in a vast indoor environment, such as a commercial facility or warehouse, and estimate their poses using a small Bicode marker.

We implemented a prototype of the proposed method and evaluated the performance of the Bicode system's 2D and blinker marker functions at various distances and marker sizes. As a result, we successfully recognized their IDs from distances exceeding $20\,\mathrm{m}$ and identified their poses from distances of approximately $2.5\,\mathrm{m}$ using a $5\,\mathrm{cm}$ square marker. Our findings revealed a correlation between the reading distance and marker size, capturing angle, and the intensity of light emitted from the marker. Notably, the system also demonstrated functionality under marker movement and in evening outdoor conditions.

II. PROPOSED METHOD

The Bicode system comprises a marker unit that incorporates 2D and blinker marker functions, along with a recognition unit with an event camera and a PC for data processing. The recognition unit processes the data captured by the event camera and converts it into an image-compatible format (Fig. 2a, 2b, 2d, and 2e). Subsequently, it identifies the pose of the 2D marker (Fig. 2c) and detects marker regions to determine the ID of the blinker marker (Fig. 2f, 2g).

A. Marker region detection

First, how to find marker regions is explained. Compared to an RGB camera that obtains an image frame by acquiring and comparing the brightness of all pixels of a sensor, an event camera acquires the brightness change asynchronously for each pixel (called event data). Consequently, to perform image processing, such as detecting blinker marker regions and recognizing 2D markers, it is necessary to convert event data into an image frame. Event data obtained from an event camera is typically represented as (x, y, p, t), where x and y are the coordinates of the pixel, p represents the polarity of the brightness change (with $p = 1$ indicating an increase, referred to as 'event ON,' -1 indicating a decrease, referred to as an 'event OFF,' and 0 indicating no change, and t is the time at which the event occurred).

The image frame at time $t + \Delta t$ can be defined as a 3-valued image by adding the value of p to the time series for the period of Δt at each coordinate where the pixel value is defined as 1 when the total value is positive, -1 when it is negative, and 0 when it is even, as shown in Fig. 3. Assuming that one processing period, as shown in Fig. 2, is defined as Δt_{whole}, the accumulation times of image frames used for detecting the 2D and blinker markers can be represented by Δt_{2D} and $\Delta t_{blinker}$, respectively. The relationship between these accumulation times can be expressed as $0 < \Delta t_{2D}, \Delta t_{blinker} \leqq \Delta t_{whole}$. To detect the marker region and minimize the impact of luminance changes other than the marker blinking, $\Delta t_{blinker}$ should be set to a value slightly higher than the blinking duration of the marker. A properly set $\Delta t_{blinker}$ results in highlighted regions exclusively within the blinker region. To eliminate the noise and enhance marker region boundaries, we apply morphological transformations. The detected regions are then tracked from frame to frame. For tracking, we used a lightweight tracking algorithm SORT [33], which relies on a Kalman filter-based approach that uses the position and size of each region's bounding box.

B. Marker pose and ID recognition

To detect the 2D marker, image frames generated using the period defined as Δt_{2D} are used. The generated image frames can be processed in the same way as a typical RGB camera image. As the 2D marker for pose recognition, a

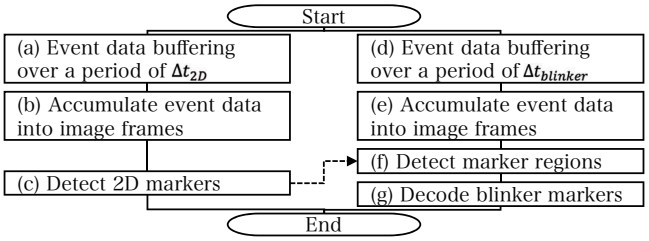

Fig. 2. Processing flow for the recognition unit: event data is converted into image frames with varying accumulation times for recognition of 2D markers (a and b) and blinker markers (d and e). If a 2D marker is recognized (c), it is used as a reference of a blinker region (f and g).

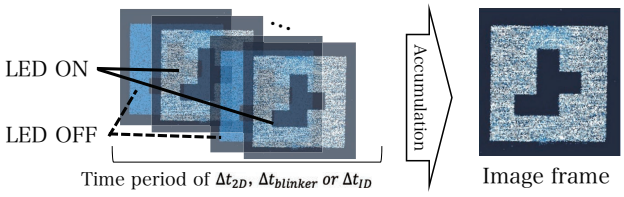

Fig. 3. Generation of image frames: event data is accumulated and synthesized in the time series to create an image frame. In this figure, white pixels represent LED ON and blue pixels represent LED OFF.

standard marker system such as ArUco [22] and ARtoolkit [21] can be employed. Since the pattern of the marker is used only for pose recognition, the pattern of the electric bulletin board may be used as a 2D marker.

Next, we describe the process of identifying the ID for detected marker regions. By performing analysis on each marker region separately, multiple markers can be recognized simultaneously. It is important to note that event cameras can capture pixels only when the brightness changes and are unable to detect LEDs that remain constantly ON or OFF. To overcome this limitation, we use Manchester coding at a frequency of f_{ID}. This coding scheme ensures that a brightness change always occurs in the expression of each blinking bit. To estimate the state of the LED from event data, we compare the total number of LED ON and OFF event pixels detected within the blinker region. This comparison is performed using the image frames accumulated over a period of Δt_{ID} seconds. Regarding the point in time, when the number of ON event pixels exceeds that of OFF event pixels, it is considered the LED ON time, and vice versa, it is considered the LED OFF time. This relationship is governed by the sampling theorem, which establishes that $0 < \Delta t_{ID} \leqq \frac{1}{2f_{ID}}$.

III. IMPLEMENTATION

A. Marker unit

We implemented the marker unit comprising an acrylic plate, a reflection tape, and a shading plate, which are used to construct the 2D marker function. In addition, an LED was inserted into the side of the acrylic plate to construct the blinker marker function, with the LED controlled by a microcomputer. While the proposed method is adaptable to various sizes and light sources, we present an example featuring a $5\,\mathrm{cm}$ square marker using a $5\,\mathrm{mm}$ diameter LED, as shown in Fig. 4. For this implementation, we used a transparent acrylic plate with $5\,\mathrm{mm}$ thickness to match

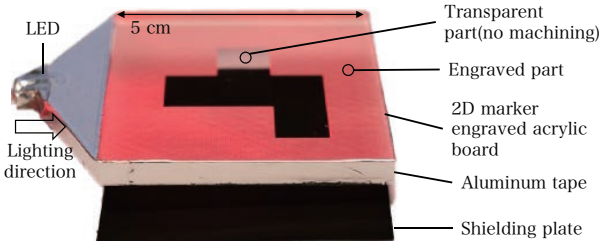

Fig. 4. Details of the Bicode marker: the LED light on the left side is diffusely reflected and only glows red at the engraved section of the marker. The transparent portion of the marker appears dark.

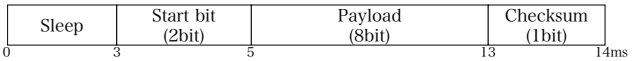

Fig. 5. Data structure of blinker markers, which comprises a start bit to divide the blinking cycle, payload, and checksum.

the diameter of the LED. A 2D marker pattern was laser-engraved into the plate, utilizing the ArUco [22] pattern. The LED light is input from the side of the acrylic plate and undergoes diffuse reflection by the engraved 2D marker pattern. Consequently, only the marker pattern appears to emit light. The selected LED, which is a $5\,\mathrm{mm}$ bullet-type with a red color, specifically model OSR5CA5B61P from OptoSupply Limited, was powered at a voltage of $5\,\mathrm{V}$.

Although the marker is primarily intended for indoor use, it may still be influenced by sunlight when used indoors. To address this issue, we incorporated an infrared (IR) LED instead of a red LED into the marker, along with an event camera equipped with an IR filter. For the IR LED, we used the OSI5LA5A33A-B model from OptoSupply Limited, which has a peak wavelength of 940 nm. In addition, we used an IR88 filter from FUJIFILM Corporation. The filter exhibits approximately $80\,\%$ transmittance at a wavelength of $940\,\mathrm{nm}$ while effectively blocking visible light. It is worth noting that sunlight at around $940\,\mathrm{nm}$, reaching the ground surface, is attenuated by the atmosphere [34]. Thus, the inclusion of LED and IR filters in the Bicode system is expected to mitigate the impact of nondirect sunlight entering the room. The LED was controlled by an XIAO RP 2040 microcomputer (Seeed K.K.) with a transistor amplifier circuit. We designed a data structure capable of transmitting 8 bits of payload within 14 ms, functioning as a blinker marker using Manchester coding at a frequency f_{ID} of $1\,\mathrm{kHz}$, as shown in Fig. 5. This marker continually transmits data in this format, achieving a bit rate of $571\,\mathrm{bps}$.

B. Recognition unit

The recognition unit was equipped with a CS-mount lens with a focal length of 8 mm, an event camera Prophesee EVK 4 (Prophesee S.A.), and a laptop PC for event data processing. The lens was configured at F2.0 to ensure sensitivity when using IR LEDs and at F5.6 to ensure image quality when using red LEDs. The combination of the Prophesee EVK 4 and an $8\,\mathrm{mm}$ focal length lens provided an approximate $40°$ angle of view in the horizontal direction. To detect 2D markers by converting event data into image frames, it was crucial to appropriately set the accumulation time Δt_{2D} for the event data and exposure time for the

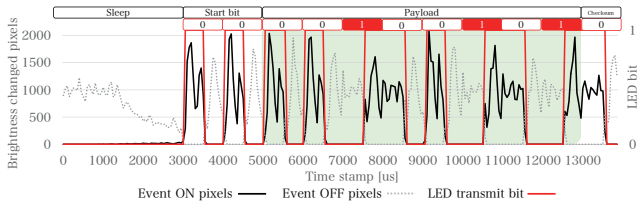

Fig. 6. This graph illustrates the correlation between the LED transmission bit (depicted in red), the total number of event ON and OFF pixels (represented by a solid black line and dashed gray line, respectively), and the Manchester code result (top of the figure). The payload data transmitted in this graph is '00100101'.

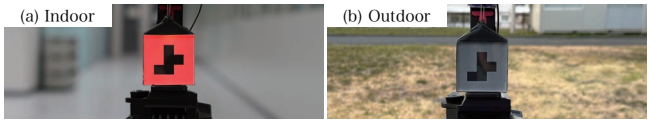

Fig. 7. Experimental conditions included (a) indoor lighting with the red LED marker and (b) outdoor lighting with the IR LED marker.

RGB camera. The Prophesee metavision SDK was used for event data processing, and the Python ArUco library was used for 2D marker recognition from image frames, with default parameters. We opted for a value of $13.2\,\mathrm{ms}$ as Δt_{2D} because it rendered the marker image discernible under indoor conditions. Conversely, for blinker marker region detection, we minimized the accumulation time $\Delta t_{blinker}$ to reduce the impact of movements other than the markers. In this implementation, we set the accumulation time $\Delta t_{blinker}$ to $2\,\mathrm{ms}$, which is the shortest duration capable of displaying the blinker marker region as a bright spot, following the structure depicted in Fig. 5. The accumulation time Δt_{ID} for recognizing blinker IDs selected was $0.25\,\mathrm{ms}$, which ensures full compliance with the conditions outlined in Section II-B. The overall processing period Δt_{whole} was established at $33\,\mathrm{ms}$ to ensure that the entire data structures shown in Fig. 5 were buffered at least once.

Fig. 6 illustrates an example of the blinker marker decoding mechanism. The decoding process for detecting the ID of the blinker marker is performed sequentially following the data structure presented in Fig. 5. This process begins with the $3\,\mathrm{ms}$ consecutive turning off of the LED.

IV. EVALUATION

Using the prototype implemented in Section III, we conducted an evaluation of the recognition performance and characteristics, considering the specifications and environmental factors related to the proposed method.

A. Current flowing through Bicode LED

As a general principle, the intensity of a point light source decreases as the square of the distance increases. As our method uses a point light source as an active marker, the marker's brightness naturally decreases with distance, adhering to the inverse square law. Thus, we investigated the relationship between the current value, which directly influences the brightness of the LED in the marker, and the recognition distance for the 2D and blinker marker functions.

The LED used in the implementation exhibits a relative brightness that is almost directly proportional to the current within the rated current range. To investigate the impact of

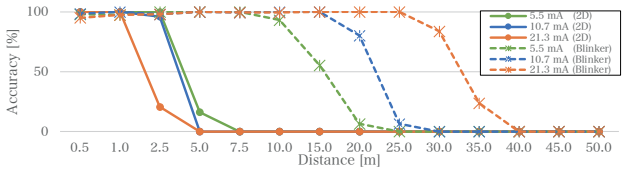

Fig. 8. The relationship between the current value applied to the LED of the marker and the recognition accuracy at each distance was analyzed.

current variations on the marker's LED, we compared the standard current of $10.7\,\mathrm{mA}$ with two different current levels: $5.5\,\mathrm{mA}$, approximately half the standard level, and $21.3\,\mathrm{mA}$, which was double the standard level. We used $5\,\mathrm{cm}$ sized marker with a red LED. The experiment was conducted in an indoor office environment with an approximate brightness of $350\,\mathrm{lx}$, as illustrated in Figure 7a.

We varied the shooting distance from 0.5 to $50\,\mathrm{m}$, with the optical axis of the camera set perpendicular to the surface of the marker. To assess the accuracy of 2D and blinker markers, we calculated the ratio of correctly identified frames to the total number of frames within the respective evaluation period. To ensure consistency, we applied the same accuracy calculation method in all subsequent experiments. In this experiment, the evaluation period was set at $6.7\,\mathrm{sec.}$ (about $200\,\mathrm{frames}$ within a $33\,\mathrm{ms}$ processing period). Since the existing ArUco library was used for 2D marker recognition, the performance depended on it. Therefore, the precise measurement of posture recognition was not carried out, and each frame was visually examined to confirm whether the axis of posture was correctly displayed.

Based on the findings presented in Fig. 8, with a current of $10.7\,\mathrm{mA}$, the 2D marker achieved a $100\,\%$ accuracy rate within a range of $2.5\,\mathrm{m}$; however, the recognition failed beyond $5\,\mathrm{m}$. In contrast, the blinker marker could be recognized at distances up to $20\,\mathrm{m}$. Notably, we also affirmed that the recognition distance increased with high-current levels. For instance, the use of a current of $21.3\,\mathrm{mA}$ enabled the recognition of IDs at distances of up to $30\,\mathrm{m}$.

Furthermore, we observed that, as a 2D marker function, the recognition distance tended to decrease with increase in current. This trend was associated with the observation that the 2D pattern within the image frame became increasingly blurred when the current exceeded the required level. Image frames presented in Fig. 13a, 13b, and 13c display the visual effects of 2D marker recognition. Under the conditions of $21.3\,\mathrm{mA}$, the 2D marker pattern appeared swollen and blurred in the image. These results emphasize that the brightness of the LED cannot be infinitely increased, highlighting the need to set an appropriate value to optimize the functionality of the 2D and blinker markers. As a 2D marker, although it seems recognizable even by a typical RGB camera, the 2D pattern may be unclear and the recognition accuracy may decrease depending on the exposure adjustment similar to that of observed in this experiment.

B. Angle between the marker and the camera

The proposed method uses a visual marker capable of recognizing 2D patterns and blinker IDs when captured from the marker plane. Nevertheless, when observed from

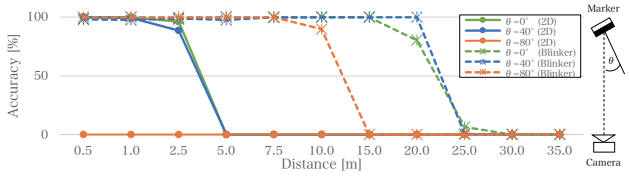

Fig. 9. The relationship between the angle θ between the marker normal and camera optical axis and the recognition accuracy at various distances.

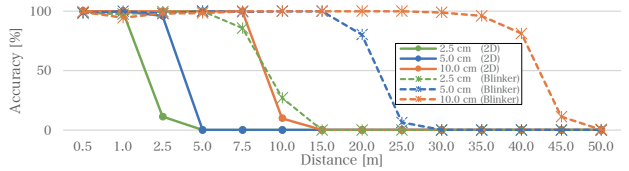

Fig. 10. The relationship between marker size and recognition accuracy at each distance.

an angle, the region of the marker visible to the camera diminishes in size. Therefore, we assessed the relationship between the capture angle and recognition distance for the 2D and blinker marker functions. In this experiment, all conditions were kept consistent with those detailed in Section IV-A, with the current of the LED set to a fixed value of $10.7\,\mathrm{mA}$. The experiment involved varying the angle between the marker and camera, specifically $0°$ (facing each other), $40°$, and $80°$, while also adjusting the distance within the range of $0.5\,\mathrm{m}$ and $35\,\mathrm{m}$.

Fig. 9 illustrates that the accuracy of the 2D marker exceeded $90\,\%$ up to a distance of $2.5\,\mathrm{m}$ when observed at angles of up to $40°$; however, it was no longer recognizable at $80°$. By contrast, the blinker marker could be recognized at distances of up to $10\,\mathrm{m}$ even at $80°$, with the recognition distance increasing as the angle decreased. Our findings suggest that a steeper angle results in reduced visibility of the features in the 2D pattern and in capturing a small marker area through the camera lens. Image frames for 2D marker recognition at each angle are presented in Fig. 13b, 13d, and 13e. The size of the marker region observed at a $0°$ is approximately $1/4$ of the size of marker at $80°$.

C. Marker size

This experiment aimed to explore the relationship between the marker size and the distance over which each 2D and blinker marker could function. We made comparisons using marker sizes of 2.5, 5, and $10\,\mathrm{cm}$, ensuring that the relative luminosity per unit area was consistent for each size. This alignment was achieved by using LED currents of 2.7, 10.7, and $40.9\,\mathrm{mA}$, respectively. All other conditions remained identical to those shown in Section IV-A.

Fig. 10 illustrates that for a 2D marker with a size of $10\,\mathrm{cm}$, the accuracy rate remained consistently at $100\,\%$ up to a distance of $7.5\,\mathrm{m}$, with the recognition distance decreasing as the marker size decreased. Similarly, for a blinker marker with a size of $10\,\mathrm{cm}$, the accuracy rate remained above $80\,\%$ up to a distance of $40\,\mathrm{m}$, with the recognition distance decreasing as the marker size decreased. This observation can be attributed to the size of the marker's image captured by the camera. Image frames presented in Fig. 13b, 13f, and 13g show the recognition process for the 2D marker at

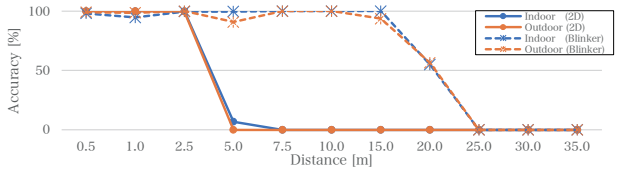

Fig. 11. Accuracy of recognizing distances indoors and outdoors using infrared markers.

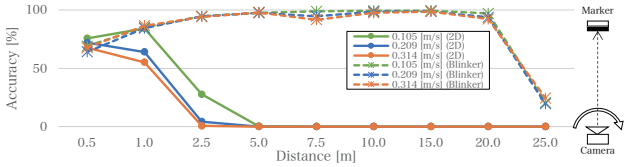

Fig. 12. Relationship between the speed of camera rotation and the accuracy of recognition at each distance.

various sizes. These results demonstrate that, at the same distance, the region of a marker reflected in the camera increases proportionally with the size of the marker. In this experiment, it was observed that even a $2.5\,\mathrm{cm}$ Bicode marker recognized the ID from $7.5\,\mathrm{m}$ and, when brought closer to $1\,\mathrm{m}$, recognized the pose.

D. Recognition in and out of the building

While the marker system is designed for indoor use, we assessed the recognizable distance of each marker function under varying ambient light conditions, thereby validating the countermeasures against sunlight implemented in Section III. Initially, we confirmed that, under outdoor conditions, the use of visible red LEDs with a $5\,\mathrm{cm}$ marker size did not enable recognition at all. The experiment took place at evening outdoor, as shown in Fig. 7b, with an ambient light level of approximately $2000\,\mathrm{lx}$, while indoor conditions maintained an ambient light level of approximately $350\,\mathrm{lx}$. Subsequently, we conducted experiments in both indoor and outdoor environments using a $5\,\mathrm{cm}$ marker size, an IR LED, and an event camera equipped with an IR filter. The LED current was set to $20.4\,\mathrm{mA}$, corresponding to the high-current condition detailed in Section IV-A. All other conditions remained consistent with those described in Section IV-A.

The results depicted in Fig. 11 reveal that the recognition accuracy for both 2D and blinker markers remained nearly $100\,\%$ up to a distance of $2.5\,\mathrm{m}$ in both indoor and outdoor environments. However, for blinker markers, the accuracy declined to roughly to $50\,\%$ at a distance of around $20\,\mathrm{m}$ in both environments. Interestingly, the results obtained under the outdoor conditions using an LED current of $20.4\,\mathrm{mA}$ were nearly equivalent to those achieved indoors with a current of 10.7 mA, as detailed in Section IV-A. However, during a sunny day around noon, the ambient light conditions reached levels in the tens of thousands of lux, rendering the marker with IR settings unable to function.

E. Translational movement of the camera

To evaluate the performance of Bicode under conditions involving camera movement, we conducted experiments under camera translation. Given the difficulty of achieving high and constant camera translation speeds, we opted to rotate the camera in one direction perpendicular to the ground

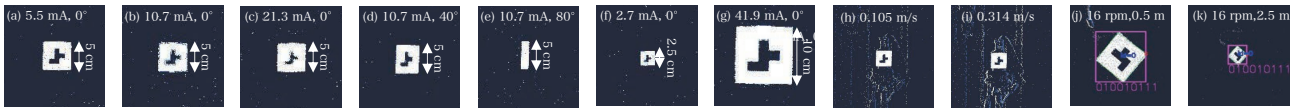

Fig. 13. (a)-(g): The generated image frames for 2D marker recognition are displayed. Those images were captured at a distance of 2.5 m, while other conditions such as LED current variations (a-c), shooting angle variations (b, d, e), and size variations (b, f, g) were also considered.
(h)-(k): The image frames used to recognize blinker markers in different camera translation and marker rotation conditions are presented. Images (h) and (i) were taken from a distance of 2.5 m at camera translation speeds of 0.105 and 0.314 m/s respectively, whereas images (j) and (k) were taken at marker rotation speeds of 16 rpm from distances of 0.5 and 2.5 m respectively.

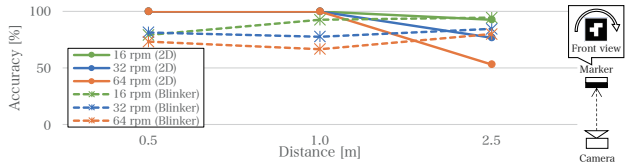

Fig. 14. The relationship between the speed of marker rotation and the accuracy of recognition at each distance.

to simulate translational motion. For this experiment, we maintained a constant tangent speed of 0.105, 0.209, and $0.314\,\mathrm{m/s}$ at each distance. The $5\,\mathrm{cm}$ marker was illuminated by a red LED with a current of $10.7\,\mathrm{mA}$, and we varied the shooting distance from 0.5 to $25\,\mathrm{m}$. The accuracy evaluation followed the same calculation method outlined in Sections IV-A through IV-D. However, in this experiment, the evaluation period extended from the time the marker entered the field of view until it disappeared.

In Fig. 12, the accuracy of the 2D marker dropped to approximately to $50\,\%$ at $1\,\mathrm{m}$ when subjected to a movement speed of $0.314\,\mathrm{m/s}$, and it became completely unrecognizable at around $2.5\,\mathrm{m}$. Notably, as the speed increased, the recognition accuracy at each distance declined. In contrast, even at a speed of $0.314\,\mathrm{m/s}$, the blinker marker maintained recognition accuracy of over $90\,\%$ at a distance of $20\,\mathrm{m}$. However, there was a decrease in accuracy in short-range recognition when compared to the camera's static condition. This phenomenon occurred because when the marker was close to the camera, the marker area appeared larger, resulting in an excessive amount of event data to process for recognition. Blinking ID recognition operates at a high rate, determined by Δt_{ID}, as described in Section III. Consequently, there was some delay in marker detection to blinker ID recognition when confronted with an abundance of event data. Additionally, shorter distances in this experiment meant shorter evaluation periods, leading to lower accuracy at close distances. In the recognition of blinker IDs, the detection of the marker region, as shown in Fig. 2f, played a crucial role, while any motion other than that of the marker was treated as noise in region detection. As seen in Fig 13h and 13i, our proposed method effectively separated the marker from the motion under the tested speed conditions. To make it more robust against motion, it is necessary to ensure that only the region that blinks at the marker frequency is extracted, while this processing may be complicated.

F. Marker rotation

We also assessed the performance of both the 2D and blinker markers under conditions where the markers themselves rotated perpendicular to the camera's optical axis. For these experiments, we used a $5\,\mathrm{cm}$ marker illuminated by a red LED with a current of $10.7\,\mathrm{mA}$, set in the same environment as described in Section IV-E. The shooting distance was varied between 0.5 and $2.5\,\mathrm{m}$, where recognition of both the 2D and blinker marker functions was confirmed under static conditions in Section IV-A. Accuracy measurements were taken during $180°$ rotation at speeds of 16, 32, and $64\,\mathrm{rpm}$.

The results presented in Fig. 14 indicate that the 2D marker achieved $100\,\%$ accuracy at distances up to $1\,\mathrm{m}$, with accuracy decreasing as both distance and rotation speed increased. At a distance of $2.5\,\mathrm{m}$, the accuracy dropped to around $50\,\%$ when the rotation speed reached $64\,\mathrm{rpm}$. In contrast, the blinker marker displayed an interesting trend; its recognition accuracy increased as the rotation speed decreased. When rotating at $64\,\mathrm{rpm}$, the blinker marker maintained a recognition accuracy of more than $70\,\%$, regardless of the distance tested. At $16\,\mathrm{rpm}$, the accuracy was more than $80\,\%$. Unfortunately, as was observed in Section IV-E, the recognition accuracy decreased as the distance between the marker and the camera decreased. Fig. 13j and 13k illustrate the recognition process using an image frame converted from event data, showing that the marker pattern remained clear at both distances, although the marker region expanded as the distance decreased.

V. CONCLUSION

In this paper, we have introduced Bicode, a versatile marker system designed for recognition using an event camera. Bicode serves as a blinker marker with a broadband ID at a distance and as a 2D marker capable of pose estimation at short ranges. Implementing Bicode is straightforward, requiring only an LED, a microcomputer for control, a battery, a transparent plate, and reflective and shading tape. Marker sizes can be adjusted by varying the amount of light emitted by the LED. Notably, the proposed method accommodates IR and red LEDs, offering flexibility in various scenarios. In the experiments, we clarified the performance of the marker type (2D and blinker) in terms of recognition distance, viewing angle, and environmental conditions. Despite some limitations, our method demonstrated effectiveness under dynamic conditions and in environments affected by sunlight. This versatile approach opens up possibilities for robotic applications, enabling rapid object identification and manipulation with small Bicode markers within large indoor spaces.

REFERENCES

[1] R. Weinstein, "Rfid: a technical overview and its application to the enterprise," *IT Professional*, vol. 7, no. 3, pp. 27–33, May 2005.

[2] S. Ting, S. Kwok, A. H. Tsang, and G. T. Ho, "The study on using passive rfid tags for indoor positioning," *International Journal of Engineering Business Management*, vol. 3, p. 8, 2011. [Online]. Available: https://doi.org/10.5772/45678

[3] L. Ni, Y. Liu, Y. C. Lau, and A. Patil, "Landmarc: indoor location sensing using active rfid," in *Proceedings of the First IEEE International Conference on Pervasive Computing and Communications, 2003. (PerCom 2003).*, March 2003, pp. 407–415.

[4] Y. Zhao, Y. Liu, and L. M. Ni, "Vire: Active rfid-based localization using virtual reference elimination," in *2007 International Conference on Parallel Processing (ICPP 2007)*, Sep. 2007, pp. 56–56.

[5] F.-j. Zhu, Z.-h. Wei, B.-j. Hu, J.-g. Chen, and Z.-m. Guo, "Analysis of indoor positioning approaches based on active rfid," in *2009 5th International Conference on Wireless Communications, Networking and Mobile Computing*, Sep. 2009, pp. 1–4.

[6] Y. Oikawa, "Tag movement direction estimation methods in an rfid gate system," in *Current Trends and Challenges in RFID*, C. Turcu, Ed. Rijeka: IntechOpen, 2011, ch. 22. [Online]. Available: https://doi.org/10.5772/18549

[7] M. Ji, J. Kim, J. Jeon, and Y. Cho, "Analysis of positioning accuracy corresponding to the number of ble beacons in indoor positioning system," in *2015 17th International Conference on Advanced Communication Technology (ICACT)*, July 2015, pp. 92–95.

[8] L. Bai, F. Ciravegna, R. Bond, and M. Mulvenna, "A low cost indoor positioning system using bluetooth low energy," *IEEE Access*, vol. 8, pp. 136 858–136 871, 2020.

[9] J. Haverinen and A. Kemppainen, "A global self-localization technique utilizing local anomalies of the ambient magnetic field," in *2009 IEEE International Conference on Robotics and Automation*, May 2009, pp. 3142–3147.

[10] A. Saxena and M. Zawodniok, "Indoor positioning system using geomagnetic field," in *2014 IEEE International Instrumentation and Measurement Technology Conference (I2MTC) Proceedings*, May 2014, pp. 572–577.

[11] B. Li, T. Gallagher, A. G. Dempster, and C. Rizos, "How feasible is the use of magnetic field alone for indoor positioning?" in *2012 International Conference on Indoor Positioning and Indoor Navigation (IPIN)*, Nov 2012, pp. 1–9.

[12] V. Pasku, A. De Angelis, G. De Angelis, D. D. Arumugam, M. Dionigi, P. Carbone, A. Moschitta, and D. S. Ricketts, "Magnetic field-based positioning systems," *IEEE Communications Surveys and Tutorials*, vol. 19, no. 3, pp. 2003–2017, thirdquarter 2017.

[13] G. Gallego, T. Delbruck, G. Orchard, C. Bartolozzi, B. Taba, A. Censi, S. Leutenegger, A. J. Davison, J. Conradt, K. Daniilidis, and D. Scaramuzza, "Event-based vision: A survey," *IEEE Transactions on Pattern Analysis and Machine Intelligence*, vol. 44, no. 01, pp. 154–180, jan 2022.

[14] D. Liu, A. Parra, Y. Latif, B. Chen, T.-J. Chin, and I. Reid, "Asynchronous optimisation for event-based visual odometry," in *2022 International Conference on Robotics and Automation (ICRA)*, May 2022, pp. 9432–9438.

[15] C. L. Gentil, I. Alzugaray, and T. Vidal-Calleja, "Continuous-time gaussian process motion-compensation for event-vision pattern tracking with distance fields," in *2023 IEEE International Conference on Robotics and Automation (ICRA)*, May 2023, pp. 804–812.

[16] D. Weikersdorfer, D. B. Adrian, D. Cremers, and J. Conradt, "Event-based 3d slam with a depth-augmented dynamic vision sensor," in *2014 IEEE International Conference on Robotics and Automation (ICRA)*, May 2014, pp. 359–364.

[17] S. Bryner, G. Gallego, H. Rebecq, and D. Scaramuzza, "Event-based, direct camera tracking from a photometric 3d map using nonlinear optimization," in *2019 International Conference on Robotics and Automation (ICRA)*, May 2019, pp. 325–331.

[18] S. Lin, Y. Zhang, D. Huang, B. Zhou, X. Luo, and J. Pan, "Fast event-based double integral for real-time robotics," in *2023 IEEE International Conference on Robotics and Automation (ICRA)*, May 2023, pp. 796–803.

[19] A. Censi and D. Scaramuzza, "Low-latency event-based visual odometry," in *2014 IEEE International Conference on Robotics and Automation (ICRA)*, May 2014, pp. 703–710.

[20] J. Rekimoto and Y. Ayatsuka, "Cybercode: Designing augmented reality environments with visual tags," in *Proceedings of DARE 2000 on Designing Augmented Reality Environments*, ser. DARE '00. New York, NY, USA: Association for Computing Machinery, 2000, pp. 1–10. [Online]. Available: https://doi.org/10.1145/354666.354667

[21] H. Kato and M. Billinghurst, "Marker tracking and hmd calibration for a video-based augmented reality conferencing system," in *Proceedings 2nd IEEE and ACM International Workshop on Augmented Reality (IWAR'99)*, Oct 1999, pp. 85–94.

[22] S. Garrido-Jurado, R. Muñoz-Salinas, F. Madrid-Cuevas, and M. Marín-Jiménez, "Automatic generation and detection of highly reliable fiducial markers under occlusion," *Pattern Recognition*, vol. 47, no. 6, pp. 2280–2292, 2014. [Online]. Available: https://www.sciencedirect.com/science/article/pii/S0031320314000235

[23] J. Wang and E. Olson, "Apriltag 2: Efficient and robust fiducial detection," in *2016 IEEE/RSJ International Conference on Intelligent Robots and Systems (IROS)*, Oct 2016, pp. 4193–4198.

[24] Y. Ayatsuka, "Fractal codes: Layered 2d codes with a self-similar layout," *Pervasive 2007 Advances in Pervasive Computing*, pp. 83–86, 05 2007.

[25] H. Sarmadi, R. Muñoz-Salinas, M. Olivares-Mendez, and R. Medina-Carnicer, "Detection of binary square fiducial markers using an event camera," *IEEE Access*, vol. 9, pp. 27 813–27 826, 01 2021.

[26] A. Mohan, G. Woo, S. Hiura, Q. Smithwick, and R. Raskar, "Bokode: Imperceptible visual tags for camera based interaction from a distance," in *ACM SIGGRAPH 2009 Papers*, ser. SIGGRAPH '09. New York, NY, USA: Association for Computing Machinery, 2009. [Online]. Available: https://doi.org/10.1145/1576246.1531404

[27] N. Matsushita, D. Hihara, T. Ushiro, S. Yoshimura, J. Rekimoto, and Y. Yamamoto, "Id cam: a smart camera for scene capturing and id recognition," in *The Second IEEE and ACM International Symposium on Mixed and Augmented Reality, 2003. Proceedings.*, Oct 2003, pp. 227–236.

[28] H. Manabe, W. Yamada, and H. Inamura, "Tag system with low-powered tag and depth sensing camera," in *Proceedings of the 27th Annual ACM Symposium on User Interface Software and Technology*, ser. UIST '14. New York, NY, USA: Association for Computing Machinery, 2014, pp. 373–382. [Online]. Available: https://doi.org/10.1145/2642918.2647404

[29] K. Ahuja, S. Pareddy, R. Xiao, M. Goel, and C. Harrison, "Lightanchors: Appropriating point lights for spatially-anchored augmented reality interfaces," in *Proceedings of the 32nd Annual ACM Symposium on User Interface Software and Technology*, ser. UIST '19. New York, NY, USA: Association for Computing Machinery, 2019, pp. 189–196. [Online]. Available: https://doi.org/10.1145/3332165.3347884

[30] K. Kim, J. Hyun, and H. Myung, *Adaptive Planar Vision Marker Composed of LED Arrays for Sensing Under Low Visibility*, 01 2019, pp. 531–540.

[31] X. Xu, Y. Shen, J. Yang, C. Xu, G. Shen, G. Chen, and Y. Ni, "Passivevlc: Enabling practical visible light backscatter communication for battery-free iot applications," in *Proceedings of the 23rd Annual International Conference on Mobile Computing and Networking*, ser. MobiCom '17. New York, NY, USA: Association for Computing Machinery, 2017, pp. 180–192. [Online]. Available: https://doi.org/10.1145/3117811.3117843

[32] A. Censi, J. Strubel, C. Brandli, T. Delbruck, and D. Scaramuzza, "Low-latency localization by active led markers tracking using a dynamic vision sensor," in *2013 IEEE/RSJ International Conference on Intelligent Robots and Systems*, Nov 2013, pp. 891–898.

[33] A. Bewley, Z. Ge, L. Ott, F. Ramos, and B. Upcroft, "Simple online and realtime tracking," in *2016 IEEE International Conference on Image Processing (ICIP)*, Sep. 2016, pp. 3464–3468.

[34] А. Стерхов and I. Loshkarev, "Determination of the proportion of natural light in solar radiation using the method of conversion of lighting units into energy," *Journal of Physics: Conference Series*, vol. 1353, p. 012002, 11 2019.